A QUASI-VEHICLE/BRIDGE INTERACTION MODEL FOR HIGH SPEED RAILWAYS

J.-D. Yau *

Department of Architecture
Tamkang University
New Taipei, Taiwan

L. Frýba

Institute of Theoretical and Applied Mechanics
ASCR, v.v.i.
Prague, Czech Republic

ABSTRACT

Vehicle response is served as a reference to evaluate riding comfort of passengers and running safety of moving carriages for high speed trains. In analyzing the vehicle-bridge interaction (VBI) problems, two sets of coupled equations of motion for running vehicles and bridge need to be solved and the VBI system matrices must be updated and factorized at each time step in a time-history analysis. This paper proposed a quasi-VBI model to abridge the complicated computational process, in which the bridge is subjected to only moving static forces of the train loadings, and the moving vehicle over it is excited by the corresponding feedback bridge response. To examine the interacting degree of the vehicle with the bridge, a coupling evaluation index (*CEI*) is defined as a quantitative assessment of the VBI system. The numerical parametric studies reveal that (1) the mass ratio of vehicle to bridge is the most sensitive parameter affecting the bridge response; (2) increasing bridge damping can reduce the coupling degree of the VBI system at high speeds; (3) the present quasi-VBI model is an efficient and simple tool to predict the vehicle's response with enough accuracy based on engineering approximation.

Keywords: High speed train, Quasi-VBI model, Resonance, Vehicle-bridge interaction, Vibration.

1. INTRODUCTION

Compared to traditional highway or air travel systems, high speed rail possesses the following superiorities: (1) relieve road and air congestion; (2) provide efficient and high capacity transportation for passengers; and (3) reduce carbon emissions in a carbon-constrained world. Obviously, high-speed rail has become a priority for medium-distant (up to 800km) intercity transportation in many countries. Among the research work of train-induced vibration problems, vehicle-bridge interaction (VBI) dynamics is of great concern in high speed rail system. In analyzing the VBI problem, two sets of equations of motion are written [1], one for the supporting bridge and the other for each of the moving vehicles over the bridge [2]. Considering the coupled system, the two sets of differential equations, in general, are solved by the following computational approaches: (1) full vehicle-bridge coupling system [3-11], (2) iterative scheme [12-15], and (3) dynamic condensation method [1,16-19]. For the full VBI models, the contact forces between the moving vehicles and the bridge vary with respect both to time and space. The system matrices, which are functions of the contact forces, must be updated and factorized at each time step in a time-history analysis. Obviously, the computing efficiency in solving the full VBI system equations would become an issue of great concern for a train consisting of a number of vehicles in connection. For this, procedures of iterative nature were adopted [12-15] by first solving the bridge equations to obtain the interaction forces and then proceeding to excite the moving vehicles at contact points for obtaining the vehicles' response. Continuing the iterative process until convergence. But the rate of convergence of iterations is likely to become low, when dealing with the situation of a bridge sustaining a large number of moving vehicles. On the other hand, condensation methods were proposed in the references [1,16-19], in which a typical technique is to condense the vehicle degrees of freedom (DOFs) to the associated bridge DOFs. Garg and Dukkipati [16] used the Guyan reduction technique (static condensation) to condense the vehicle degrees of freedom (DOFs) to the associated bridge DOFs. In the paper by Yang and Lin [17], the dynamic condensation method was used to eliminate all the vehicle DOFs on the element level. These methods have been demonstrated to be efficient for computing the bridge response. By using the Newmark finite difference scheme to discretize the vehicle equations, rather accurate bridge-vehicle relations have been established and used in eliminating the vehicle DOFs from the bridge equations [18,19], in which both the vehicle and bridge response can be computed accurately. All of these methods need intensive computations to perform updating and factorization of system matrices at each time step in dynamic response analysis.

From an engineering viewpoint, a high speed railway bridge should be designed to provide sufficient structural strength and safety for a train moving over it with

* Corresponding author (jdyau@mail.tku.edu.tw)

DOI : 10.1017/jmech.2014.89
Copyright © 2015 The Society of Theoretical and Applied Mechanics, R.O.C.
https://doi.org/10.1017/jmech.2014.89 Published online by Cambridge University Press

high speeds. Therefore, the maximum acceleration of a train traveling on a bridge is strictly limited in 0.1g [20] because of running safety and riding comfort of the train. By this strict requirement, we can assume the moving vehicle-induced vertical inertial force acting on the bridge is negligible [21] and the bridge is subjected to only sequential moving static forces of the train loadings. By solving the equation of motion of the bridge analytically, the dynamic response of the vehicle excited by the feedback bridge response can be computed. This study calls such an approach as quasi-VBI decomposition method and the decoupled vehicle-bridge system as quasi-VBI model. Although the quasi-VBI decomposition method is a simple and efficient way to analyze interaction dynamics of train/bridge coupling system, few literatures investigated the computational accuracy and feasibility of the quasi-VBI model applied to VBI problems.

By considering the vehicle and bridge system with full coupled equations as a real-VBI system, the parametric studies, including mass ratio of vehicle to bridge, suspension system, and rail irregularity, are carried out to verify the feasibility of the present quasi-VBI model to simulate interacting behavior of VBI dynamics. Moreover, this study defines a coupling evaluation index (*CEI*) to indicate the interacting extent of a VBI system. Numerical investigations show that the mass ratio of vehicle to bridge over 10% affects the bridge response significantly and increasing bridge damping can reduce the coupling degree of the VBI system at high speeds.

2. EQUATIONS OF MOTION FOR THE VEHICLE-BRIDGE SYSTEM

As shown in Fig. 1, a train is crossing a bridge. Because of regular and repetitive nature of wheel loads, the train model can be regarded essentially as a series of sprung mass units moving over a simply supported beam. The sprung mass unit is composed of a sprung mass (m_v) and an unsprung mass (m_w) interconnected by a spring-dashpot system (see Fig. 2). To analyze the train-bridge interaction dynamics, appreciable simplifications are outlined as follows [3]:

1. The bridge is modeled as a linear elastic Bernoulli-Euler beam with uniform cross section;
2. The train passing over the simple beam is simulated as a sequence of identical sprung mass units moving at constant speed (v), in which the coupling action provided by the bogie and wheel-set as well as the rocking motion of the vehicle are neglected;
3. The sprung mass unit is used to model either the front or rear half of a carriage;
4. The unsprung mass (m_w) of the sprung mass unit always keeps in contact with the beam; and
5. The frequency of the sprung mass unit would not match with the bridge frequency for the present VBI model [27].

The equation of motion for a simple beam carrying multiple moving sprung mass units can be expressed as [3]

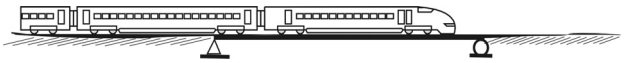


Fig. 1 Schematic diagram of a train moving over a bridge.

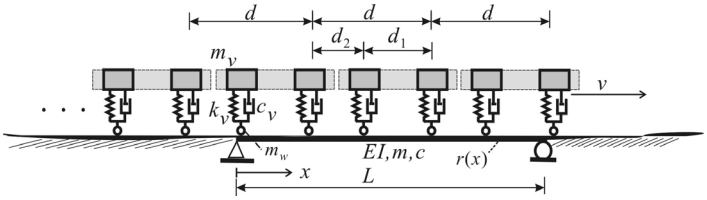


Fig. 2 Mathematical model of the simplified VBI system.

$$m\ddot{u} + c\dot{u} + EIu'''' = p(x,t)\,, \tag{1}$$

with the following homogeneous boundary conditions

$$u(0,t) = u(L,t) = 0\,, \quad EIu''(0,t) = EIu''(L,t) = 0\,, \tag{2}$$

where $(\bullet)' = \partial(\bullet)/\partial x$, $(\dot{\bullet}) = \partial(\bullet)/\partial t$, m = mass of the beam unit length along x-axis, c = damping coefficient, $u(x, t)$ = vertical deflection of the beam, EI = flexural rigidity of the beam, L = length of the beam, and $p(x, t)$ = loading function of moving oscillators. Let the sprung mass unit has the following properties: m_w = lumped mass of wheel-bogie set, m_v = lumped mass of a half carriage, c_v = equivalent damping coefficient, and k_v = equivalent suspension stiffness coefficient. Considering the regular nature of sequential sprung mass units shown in Fig. 2, the load function $p(x, t)$ shown in Eq. (1) is given by [14]:

$$\begin{aligned} p(x,t) = \sum_{k=1}^{N} & \left(P - m_v \ddot{u}_{vk} - m_w \frac{d^2u}{dt^2} \right) \\ & \delta(x - x_k) \left[H(t - t_k) - H\left(t - t_k - \frac{L}{v} \right) \right] \\ & \frac{d^2u}{dt^2} = \frac{\partial^2 u}{\partial t^2} + 2v\frac{\partial^2 u}{\partial t \partial x} + v^2 \frac{\partial^2 u}{\partial x^2} \approx \frac{\partial^2 u}{\partial t^2} = \ddot{u}\,, \end{aligned} \tag{3}$$

$$\begin{aligned} & m_v \ddot{u}_{vk} + c_v \dot{u}_{vk} + k_v u_{vk} \\ & = \begin{cases} k_v \left[u(x_k, t) + \gamma(x_k) \right] + c_v \dot{u}(x_k, t) & 0 \le x_k \left(= v(t - t_k) \right) \le L \\ k_v \gamma(x_k) & x_k < 0\,, \quad x_k > L \end{cases}, \end{aligned} \tag{4}$$

in which, $P = (m_v + m_w)g = M_v g$ = lumped weight of a moving oscillator, M_v = lumped mass of the sprung mass unit, g = gravity acceleration, δ = Dirac's delta function, $H(t)$ = unit step function, k = 1, 2, 3,…, N-th moving load on the beam, t_k = arrival time of the kth oscillator entering the beam, u_{vk} = vertical displacement of the kth lumped mass, f_{vk} = interaction force existing between the beam and the wheel mass of the k-th moving oscillator, $\gamma(x_k)$ = track irregularity (vertical profile), and x_k = position of the k-th load along the rail line, as defined in Eq. (4). Here, $x_k < 0$ represents the kth os-

https://doi.org/10.1017/jmech.2014.89 Published online by Cambridge University Press

cillator is entering to the beam, $0 \le x_k\ (= v(t-t_k)) \le L$ running on the beam, and $x_k > L$ departing from the beam. In Eq. (3), since the Coriolis $(= 2vu'm_w)$ and centrifugal $(= m_w v^2 u'')$ forces, generally, are far smaller than the inertial one, *i.e.*, $m_w\ddot{u}$ for a moving object over a stiff beam, they will be neglected in the following formulation.

As shown in Eq. (4), if the beam responses of $(u(x,t), \dot{u}(x,t))$ were computed (known), they could be regarded as exciting sources to exert the sprung mass units moving on the beam. For high speed trains, the vertical acceleration of a moving train is limited in $0.1g$ or less $0.05g$ [20]. Inspired by this, the coupling equations of Eq. (1) and (4) can be decomposed into two independent differential equations if the approximation of $P - m_v\ddot{u}_{vk} - m_w\ddot{u}(x_k,t) \approx P$ is assumed. Such an approximation to separate the VBI coupling equations is called quasi-VBI decomposition method. A detailed derivation for the proposed VBI model using the quasi-VBI decomposition method will be conducted later in Section 3.

3. DECOMPOSITION OF THE VEHICLE-BRIDGE COUPLING SYSTEM

Considering the homogenous boundary conditions shown in Eq. (2) for a simply supported beam, the dynamic deflection $u(x, t)$ in Eq. (1) can be approximated by [15,16]:

$$u(x,t) = \sum_{n=1} q_n(t) \sin\frac{n\pi x}{L}, \tag{5}$$

where $q_n(t)$ means the generalized coordinate associated with the n-th assumed mode of the simple beam. By Galerkin's method [15], the generalized equations of motion for the n-th modal system carrying multiple sprung masses moving on the beam are given as:

$$\begin{bmatrix} 1+\rho_w \sin\frac{\pi x_k}{L}\sum_{k=1}^{N}\psi_{1,k}(\varpi_1,t) & \cdots & 1+\rho_w \sin\frac{n\pi x_k}{L}\sum_{k=1}^{N}\psi_{1,k}(\varpi_1,t) & \cdots \\ \vdots & \ddots & \vdots & \vdots \\ 1+\rho_w \sin\frac{\pi x_k}{L}\sum_{k=1}^{N}\psi_{n,k}(\varpi_n,t) & \cdots & 1+\rho_w \sin\frac{n\pi x_k}{L}\sum_{k=1}^{N}\psi_{n,k}(\varpi_n,t) & \cdots \\ \vdots & \cdots & \vdots & \ddots \end{bmatrix} \begin{Bmatrix} \ddot{q}_1 \\ \vdots \\ \ddot{q}_n \\ \vdots \end{Bmatrix}$$
$$+ \begin{bmatrix} 2\xi_1\omega_1 & 0 & 0 & 0 \\ 0 & \ddots & 0 & 0 \\ 0 & 0 & 2\xi_n\omega_n & 0 \\ 0 & 0 & 0 & \ddots \end{bmatrix} \begin{Bmatrix} \dot{q}_1 \\ \vdots \\ \dot{q}_n \\ \vdots \end{Bmatrix} + \begin{bmatrix} \omega_1^2 & 0 & 0 & 0 \\ 0 & \ddots & 0 & 0 \\ 0 & 0 & \omega_n^2 & 0 \\ 0 & 0 & 0 & \ddots \end{bmatrix} \begin{Bmatrix} q_1 \\ \vdots \\ q_n \\ \vdots \end{Bmatrix}$$
$$+ \rho_v \begin{Bmatrix} \sum_{k=1}^{N}\left[\psi_{1,k}(\varpi_1,t)\times\ddot{u}_{vk}\right] \\ \vdots \\ \sum_{k=1}^{N}\left[\psi_{n,k}(\varpi_n,t)\times\ddot{u}_{vk}\right] \\ \vdots \end{Bmatrix} = \frac{2P}{mL} \begin{Bmatrix} \sum_{k=1}^{N}\psi_{1,k}(\varpi_1,t) \\ \vdots \\ \sum_{k=1}^{N}\psi_{n,k}(\varpi_n,t) \\ \vdots \end{Bmatrix} \tag{6a}$$

Equation (6a) is coupled with the following equation of motion of the sprung mass unit running on the beam

$$m_v\ddot{u}_{vk} + c_v\left(\dot{u}_{vk} - \sum_{n=1}\dot{q}_n(t)\sin\left(\frac{n\pi x_k}{L}\right)\right) + k_v\left(u_{vk} - \sum_{n=1} q_n(t)\sin\left(\frac{n\pi x_k}{L}\right)\right) = k_v\gamma(x_k)$$
$$0 \le x_k\ (= v(t-t_k)) \le L \tag{6b}$$

where $\rho_w = 2m_w/mL$, $\xi_n = c/2m\omega_n$ = modal damping ratio, $\rho_v = 2m_v/mL$, and $\omega_n = (n\pi/L)^2\sqrt{EI/m}$ = n-th natural frequency, and

$$\psi_{n,k}(\varpi_n,t) = \sin\varpi_n(t-t_k)\left[H(t-t_k) - H(t-t_k-L/v)\right],$$
$$\varpi_n = n\pi v/L \tag{7}$$

As shown in Eqs. (6a) and (6b), all the generalized equations of the beam are coupled with the differential equations of each of the sprung mass units moving over it. Thus this study calls the VBI model considering all the coupled equations as "real-VBI system". By regarding the vertical inertia force of $m_v\ddot{u}_{vk} + m_w\ddot{u}(x_k,t)$ in Eq. (1) as an external force, the n-th modal equation of motion in Eq. (6a) is rewritten as

$$\ddot{q}_n + 2\xi_n\omega_n\dot{q}_n + \omega_n^2 q_n = \frac{2P}{mL}\sum_{k=1}^{N}(1-\chi_k)\psi_{n,k}(\varpi_n,t),$$
$$\chi_k = \frac{1}{P}\left(m_v\ddot{u}_{vk} + m_w\sum_{i=1}\ddot{q}_i(t)\sin\frac{i\pi x_k}{L}\right) \tag{8}$$

where the dynamic factor χ_k represents the coupling degree of interaction of the VBI system. For high

https://doi.org/10.1017/jmech.2014.89 Published online by Cambridge University Press

speed railway bridges, generally, the vehicle's suspension system is designed to provide sufficient vibration mitigation for riding comfort of sitting passengers, and the vertical acceleration of the moving carriage is limited in 0.1*g* [20] or less 0.05*g*. Considering the strict requirement, the dynamic factor χ_k in Eq. (8) is assumed so small that it can be neglected, *i.e.*, $\chi_k \approx 0$. Therefore, the *n*-th modal equation of motion of the coupled equation shown in Eq. (6a) is further simplified as:

$$\ddot{q}_n + 2\xi_n \omega_n \dot{q}_n + \omega_n^2 q_n \approx \frac{2P}{mL}\sum_{k=1}^{N}\psi_{n,k}(\varpi_n, t), \tag{9}$$

By this approximation, the vehicle-bridge coupling system are separated into two decoupled subsystems, in which the bridge is subjected to only sequential moving static forces of the train loadings, and the *k*-th vehicle running on the beam is stimulated by the feedback beam response independently computed from Eq. (9). Once the *n*-th generalized coordinate $q_n(t)$ shown in Eq. (9) is solved (known), the beam responses under the *k*-th sprung mass unit, *i.e.*, $u(x_k, t) = \sum q_n(t)\sin(n\pi x_k / L)$ and $\dot{u}(x_k, t) = \sum \dot{q}_n(t)\sin(n\pi x_k / L)$, can be regarded as a feedback exciting force to exert the sprung mass. Thus Eq. (4) can be rewritten as follow:

$$m_v \ddot{u}_{vk} + c_v \dot{u}_{vk} + k_v u_{vk} = \begin{cases} f_{v,k} & 0 \le x_k \left(= v(t - t_k)\right) \le L \\ k_v \gamma(x_k) & x_k < 0, \quad x_k > L \end{cases}$$

$$f_{v,k} = k_v\left[\gamma(x_k) + \sum_{n=1} q_n(t)\sin\left(\frac{n\pi x_k}{L}\right)\right] + c_v \sum_{n=1}\dot{q}_n(t)\sin\left(\frac{n\pi x_k}{L}\right) \tag{10}$$

where $f_{v,k}$ represents exciting input to act on the *k*th sprung mass as it passes through the vibrating beam. Solving the vehicle's equation in Eq. (10) yields approximate response of the moving vehicle. In the following section, the feasibility and accuracy of the quasi-VBI model applied to VBI dynamics of high speed rail will be demonstrated.

4. NUMERICAL VERIFICATIONS AND PARAMETRIC ANALYSIS

As indicated in Eq. (8), the dynamic factor χ_k represents the coupling degree of interaction of a VBI system. The larger the factor χ_k, the more coupling the VBI system will be. To examine the interacting degree for a VBI system, a coupling evaluation index denoted as *CEI* is defined as:

$$CEI = |\chi_k|_{\max} = \left.\frac{\left|m_v \ddot{u}_{vk} + m_w \ddot{u}(x_k, t)\right|_{\max}}{M_v g}\right|_{M_v = m_v + m_w} \tag{11}$$

As shown in Eq. (11), the larger the *CEI*, the more important the vehicle-bridge interaction will be. Then one can adopt the *CEI* factor to evaluate the feasibility of the quasi-VBI model proposed in Section 3 to simulate a real VBI system.

To account for the random nature and characteristics of track irregularity in practice, the power spectrum density (PSD) function for track class 6 designed by Federal Railroad Administration (USA) [2] will be adopted to simulate the vertical profile of track geometry variations:

$$S(\Omega) = \frac{A_v \Omega_c^2}{(\Omega^2 + \Omega_r^2)(\Omega^2 + \Omega_c^2)} \tag{12}$$

where Ω = spatial frequency, and A_v, (= 1.5×10^{-7}m) Ω_r (= 2.06×10^{-6}rad/m), and Ω_c (= 0.825rad/m) are relevant parameters. Figure 3 shows the vertical profile of track irregularity for simulation of track geometry variations in this study.

As shown in Fig. 2, a train consists of *five* identical railway carriages with equal length *d* and each carriage is simulated by the front and rear sprung mass units with regular axle intervals d_1 and d_2, respectively Let the train cross the simply supported beam at constant speed *v*. The properties of the beam and sprung mass unit are listed in Tables 1 and 2, respectively. Here the *equivalent* suspension stiffness and damping are consider for the sprung mass unit [26,27], and the symbol of f_1 represents the first natural frequency and $v_{res,1}$ (= $f_1 d$) the first resonant speed [22-25]. Since the use of 16 modes is sufficient to describe the dynamic acceleration of a simple beam, the same number of modes will be used in all the examples to follow.

4.1 Resonance of Acceleration Response

Whenever the passage frequency (= *v*/*d*) of train loadings with identical intervals *d* matches the fundamental frequency (f_1) of the bridge, the bridge will be set in resonance [22]. From Table 2, the first resonant speed of the sequential moving loads is equal to: $v_{res,1} = f_1 d$ (= 104m/s = 375km/h). For demonstration, we shall let the sequential sprung mass units pass through the beam with smooth surface at the resonant speed (= $v_{res,1}$). Figure 4 depicts the time-history acceleration response at the midpoint of the beam computed by the quasi-VBI model (see Eqs. (9) and (10)) and the real-VBI system (see Eqs. (4) and (6)), respectively. As expected, both the acceleration responses continue to build up as there are more train loadings passing through the beam. In addition, the time-history responses of vertical acceleration for the front sprung mass of both the 1-st and 5-th carriages have been drawn in Fig. 5, respectively. Due to the resonant phenomenon occurring in the vibrating beam, the dynamic response of the front sprung mass of the 5-th carriage has been magnified significantly. Meanwhile, Fig. 6 illustrates the maximum acceleration ($a_{\max}$) at midpoint of the beam against train speed (*v*) ranged from 100km/h to 500km/h. This plot is denoted as "$a_{\max}$-*v* plot" in this study. Figure 7 depicts the maximum acceleration of the sprung masses ($a_{v,\max}$) versus the speed (*v*), which is called $a_{v,\max}$-*v* plot in the following examples. From the numerical predictions shown in Figs. 6 and 7, the present quasi-VBI model

https://doi.org/10.1017/jmech.2014.89 Published online by Cambridge University Press

Table 1 Properties of the beam.

L (m)	EI (kN-m^2)	ξ_n	m (t/m)	f_1 (Hz)
32	2.57×10^8	0.05	37.6	4.01

Table 2 Properties of the sprung mass unit.

N	m_v (t)	m_w (t)	$P = M_v g$ (kN)	k_v (kN/m)	c_v (ξ_v) (kN-s/m)	d_1 (m)	d_2 (m)	$d = (d_1 + d_2)$ (m)	f_v (Hz)	$v_{res,1}$ (km/h)
10	25	5	294	1800	10 (2.3%)	17.5	8.5	26	1.35	375

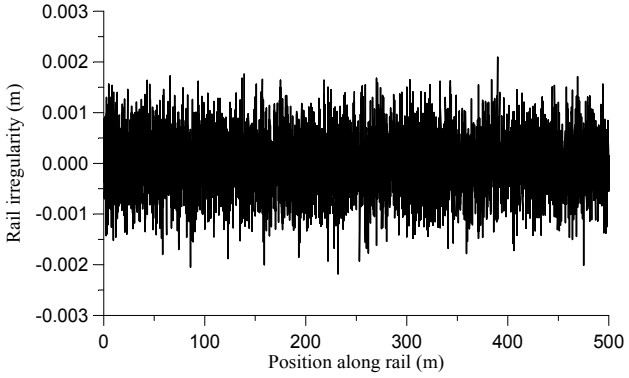


Fig. 3 Rail irregularatity (vertical profile).

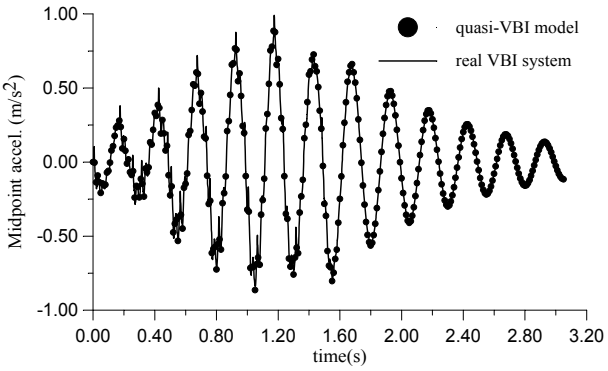


Fig. 4 Time history resonant response of midpoint acceleration of the beam.

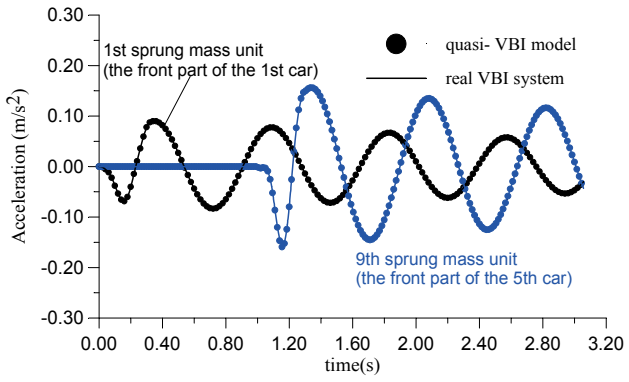


Fig. 5 Time history response of acceleration of sprung masses.

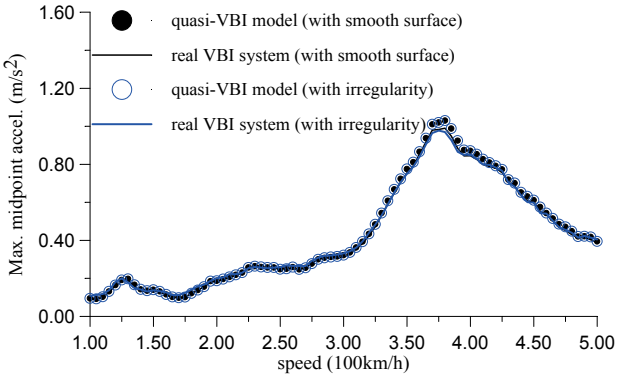


Fig. 6 a_{max}-v plot for the beam.

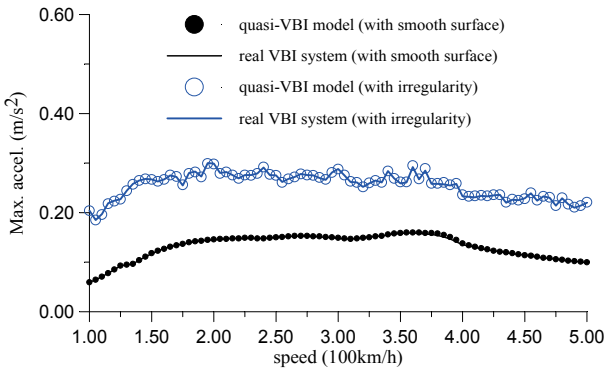


Fig. 7 $a_{v,max}$-v plot for the sprung masses.

has ability to simulate dynamic behaviors of a VBI system. This conclusion is consistent with the findings of Liu *et al*. [10] for bridge response. On the other hand, a high speed railway bridge must be designed to provide sufficient running safety and enough structural strength for a train moving over it at high speeds. According to the regulations of high speed rail, the maximum vertical acceleration of moving trains should be limited in 0.1g [20]. Consequently, by neglecting dynamic interactions of a moving train with rail bridges, the quasi-VBI decomposition method is a simple and efficient way to perform VBI dynamic analysis for simplifying engineering calculations. In practice, rail irregularities play an important role in affecting dynamic response of a VBI system. Let us introduce the rail unevenness shown in Fig. 3 into the VBI system [2], the numerical results of corresponding a_{max}-v plot and $a_{v,max}$-v plot have been also depicted in Figs. 6 and 7, respectively. It is shown that the rail unevenness results in a significant amplification on the vehicle's response, but little influence on the beam because of strict requirements of track irregularities for running safety of high speed trains. In the following examples, parametric analysis, including mass ratio of vehicle to bridge, suspension system, and rail irregularity, will be performed to evaluate the applicability of the quasi-VBI model to VBI dynamics.

4.2 Effect of Mass Ratio of Vehicle to Bridge

To evaluate the computational accuracy using the present quasi-VBI model, the properties of the sprung mass unit listed in Table 2 are used in the following examples. Let us assume the natural frequencies and

https://doi.org/10.1017/jmech.2014.89 Published online by Cambridge University Press

damping ratio of the simple beam shown in Fig. 2 remain the same as Table 1. By considering the following mass ratios of sprung mass unit to beam, *i.e.*, M_v / mL = 0.05, 0.1, and 0.15, the response curves of the $a_{\max}$-v and $a_{v,\max}$-v plots are drawn in Figs 8 and 9, respectively. Figure 8 shows the beam response curves of $a_{\max}$-v plot with the mass ratios of 0.1 or 0.15 at the resonant speed ($v_{res,1}$ = 375km/h) appear a considerable reduction of acceleration amplitude for the real-VBI system compared with the quasi-VBI model. The reduction degree of peak response at the primary resonant speed for these two VBI models are 8%, 15%, and 26% for the mass ratios with 0.05, 0.1, and 0.15, respectively. From this, the vibration reduction of the beam response is caused by the tuning effect of the sprung masses moving on the beam. It means the dynamic forces induced by moving sprung masses need to be taken into account as a heavy train travels over a light bridge. For example, as a heavier train crosses a light bridge (M_v / mL = 0.15) at resonant speed, the contribution of dynamic factor χ_k shown in Eq. (9) to the response of the bridge becomes significant in VBI dynamic analysis. Figure 9 depicts the relation of maximum acceleration ($a_{v,\max}$) of sprung masses against speed (v). As can be seen, increasing the vehicle/bridge mass ratio (M_v / mL) results in significant amplification on the vehicle's response, but has negligible computational errors between the present quasi-VBI model and the real-VBI system.

To examine the interacting degree of moving vehicle with the bridge, Fig. 10 plots the relationship of *CEI vs.* train speed (v). The numerical comparisons show that the *CEI* predicted by both the quasi-VBI and real-VBI models are in well agreement with each other except for the speed faster than 350km/h. This feature represents the quasi-VBI model is useful to simulate the dynamic behaviors of moving vehicles for VBI system. On the other hand, Fig. 10 indicates that the *CEI* curves rise with the increase of the vehicle/bridge mass ratio (M_v / mL). It represents the interacting phenomenon of heavy vehicles passing a bridge has to be taken into account in performing VBI analysis if bridge response is of concern in design.

4.3 Effect of Suspension Vertical Stiffness

In this example, let us consider the influence of suspension stiffness (k_v) on the VBI interaction dynamics. By considering the following suspension stiffness $0.5k_v$, k_v, and $3k_v$ for the sprung mass units shown in Fig. 2, which are corresponding to the frequencies of 0.95Hz, 1.35Hz, and 2.34Hz, the $a_{\max}$-v and $a_{v,\max}$-v plots of the beam and sprung mass units are depicted in Figs. 11 and 12, respectively. As the $a_{\max}$-v plot shown in Fig. 11, the quasi-VBI model cannot reflect dynamic interacting phenomenon of a real VBI system because the beam is subject to only moving static forces of the train loadings. On the other hand, Fig. 12 indicates increasing suspension stiffness may result in a significant amplification on the $a_{v,\max}$-v plot of the vehicle response, which means higher suspension vertical stiffness would not be preferred to affecting riding quality of moving carriages.

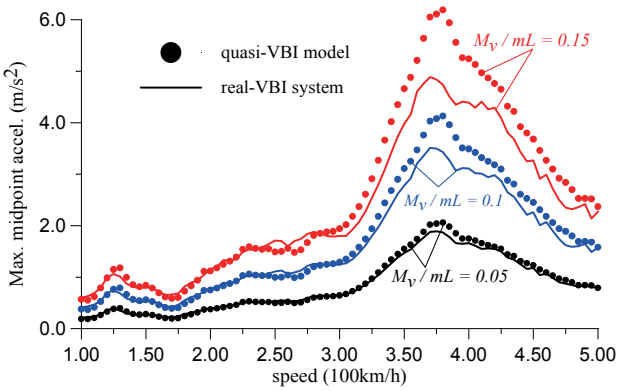


Fig. 8 Effect of mass ratio (M_v / mL) on $a_{\max}$-v plot of the beam.

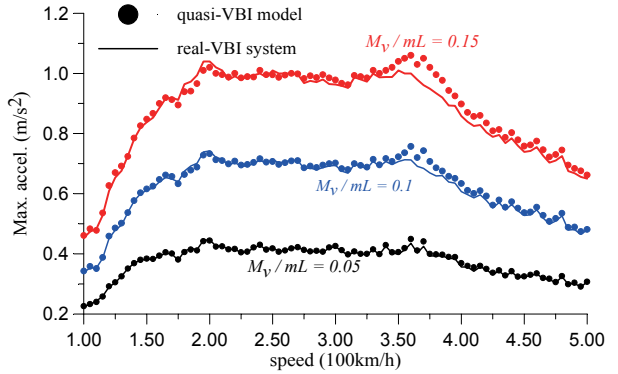


Fig. 9 Effect of mass ratio (M_v / mL) on $a_{v,\max}$-v plot of the sprung masses.

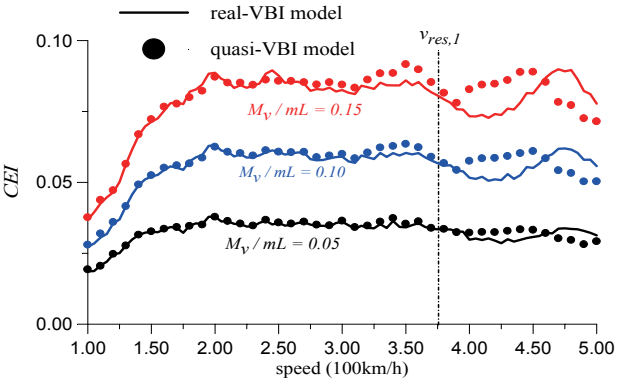


Fig. 10 Coupling degree between vehicle and bridge.

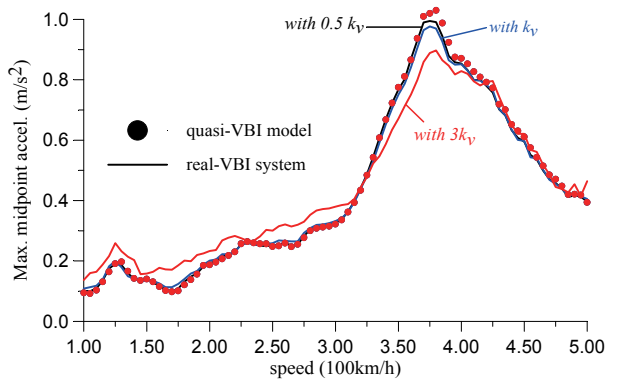


Fig. 11 Effect of suspension stiffness (k_v) on $a_{\max}$-v plot of the beam.

https://doi.org/10.1017/jmech.2014.89 Published online by Cambridge University Press

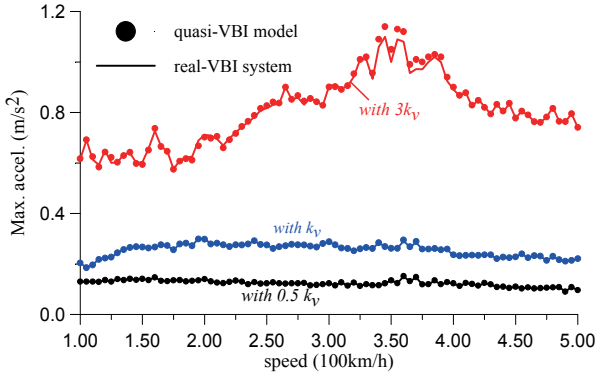


Fig. 12 Effect of suspension stiffness (k_v) on $a_{v,\max}$-v plot of the sprung masses.

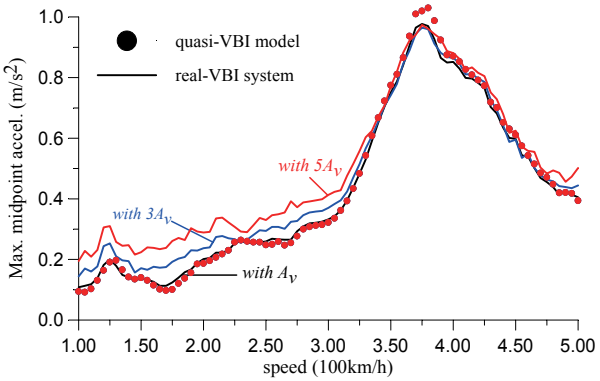


Fig. 13 Effect of rail irregularity on $a_{\max}$-v plot of the beam.

4.4 Effect of Rail Irregularities

For the purpose of comparison, the following amplitude of track irregularities are considered: A_v, $3A_v$, and $5A_v$ in this parametric analysis. Figures 13 and 14 show the $a_{\max}$-v and the $a_{v,\max}$-v plots for the VBI system given in Section 4.1, respectively. As expected, the vehicle response curve (see Fig. 14) rises with respect to the increase of amplitude of track irregularities, but significant computational errors appear on the $a_{\max}$-v plot at lower speeds, as shown in Fig. 13, for the bridge response computed by using the quasi-VBI model. The reason is that the quasi-VBI model cannot account for the amplification effect of rail irregularities on the beam response as the sequential sprung mass units move on the beam. By contrast, the quasi-VBI model can accurately predict the vehicle's response, as shown in Fig. 14. It can be explained that the track irregularities with larger amplitudes play a more decisive component than the bridge response to excite the vehicle in a feedback way. On the other hand, since the irregularities used herein are of high frequency and the suspension system considered in Table 2 is of low frequency, that is the reason why the quasi VBI is useful to predict vehicle responses. It is concluded that as a train equipped with better isolation devices travels on a railway bridge with very poor track irregularities, the interaction force due to bridge response may become a minor factor to act on the moving vehicles. For this case, the quasi VBI model is applicable to simulate the dynamic behavior of moving vehicles but inapplicable to bridge.

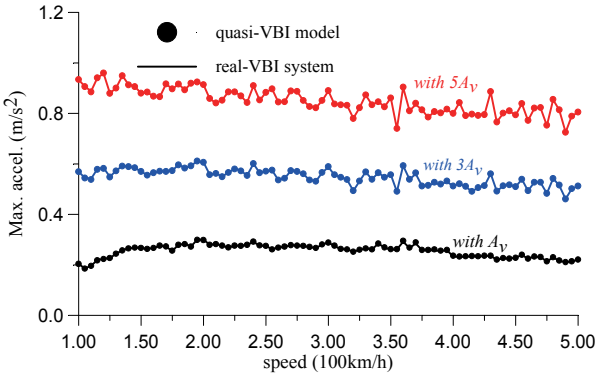


Fig. 14 Effect of rail irregularity on $a_{v,\max}$-v plot of the sprung masses.

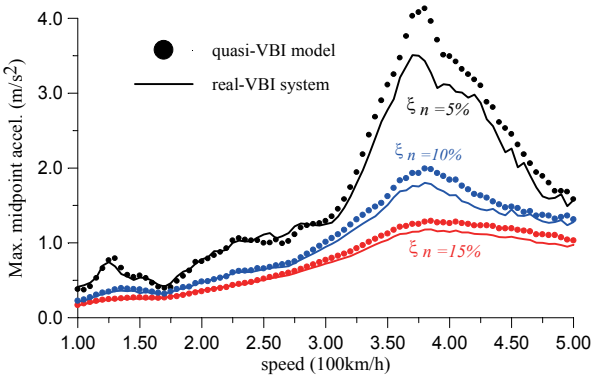


Fig. 15 Effect of bridge damping on $a_{\max}$-v plot of the beam.

4.5 Effect of Bridge Damping

In this example, let us consider the following damping ratios for the beam model: 5%, 10%, and 15%, respectively. Here, the high bridge damping ratio over 5% is employed to model a bridge equipped with dissipating devices for vibration reduction. With the mass ratio of $M_v / mL = 0.1$, the $a_{\max}$-v and $a_{v,\max}$-v plots for the beam and sprung masses have been depicted in Figs. 15 and 16, respectively. An observation indicates that increasing the damping ratio of bridges not only mitigates the bridge response of the VBI system, but also reduces the coupling degree of the VBI system at higher

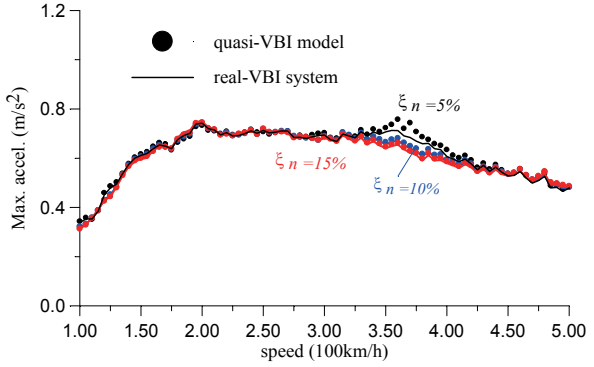


Fig. 16 Effect of bridge damping on $a_{v,\max}$-v plot of the sprung masses.

https://doi.org/10.1017/jmech.2014.89 Published online by Cambridge University Press

speeds (see Fig. 17). Moreover, the proposed quasi VBI model almost can simulate the dynamic interacting behavior of the moving rail vehicles over a bridge (see Fig. 16). It is significant for bridge designers to simplify the complex computational procedure of VBI problems using the quasi-VBI model through the increase of bridge damping.

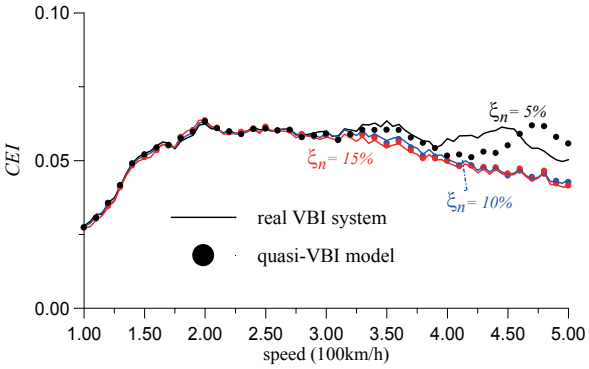


Fig. 17 Ffect of bridge damping on *CEI* of a VBI system.

5. CONCLUSIONS

Generally, high speed railway bridges are designed to be stiffener than conventional ones. Thus the quasi-VBI decomposition method is a simple and efficient approach to predict dynamic response of vehicle-bridge system for high speed rails. The proposed coupling evaluation index (*CEI*) gives a quantitative indicator to a VBI system. From the parametric analysis, the *CEI* values computed by either the quasi-VBI model or the real-VBI system are in well agreement with each other. It means the bridge response computed using the quasi-VBI model can be employed as an exciting source to exert the vehicles moving on the bridge for computing vehicle's response. On the other hand, the higher *CEI* value represents the VBI dynamics need to be taken into account in computing the beam response. By the present numerical investigations, the following conclusions can be extracted from the parametric studies of the VBI problem:

1. For small mass ratios ($M_v / mL \leq 0.05$), the quasi-VBI model can simulate the dynamic behaviors of a real-VBI system accurately. But it is inapplicable to the VBI system with the mass ratio (M_v / mL) over 10% since the bridge responses are overestimated.
2. For the case of a vehicle with stiffener suspension system, the quasi-VBI decomposition procedure fails to perform VBI dynamic analysis for bridge response.
3. Once a train travels on railway with very poor track irregularities, the feedback response from the bridge to the vehicle becomes minor excitations. Therefore, the quasi VBI model is useful to predict the dynamic response of moving vehicles but not suitable for the bridge response induced by a moving train.
4. Increasing bridge damping can reduce the coupling degree of a VBI system for bridge response so that the quasi-VBI model can be applied to VBI problems.
5. As the parametric studies shown in the sub-sections 4.2 and 4.4, the distribution of the *CEI* factor is related to mass ratio of vehicle to bridge, bridge damping, and moving speed, it seems difficult to introduce a guideline that can identify completely coupling degree of a real VBI system. Even so, the proposed quasi-VBI approach still possesses enough accuracy in predicting the dynamic responses of a VBI system for high speed rails.

ACKNOWLEDGEMENTS

The research was supported by the National Science Council in Taiwan through the Grant NSC 102-2923-E-032-002-MY3 and by the Grant Agency of the Czech Republic by the grant number 103/08/1340 and by the research project of the Institute of Theoretical and Applied Mechanics No. AVOZ 20710524 in Czech Republic.

REFERENCES

1. Yang, Y. B. and Yau, J. D., "Vehicle-Bridge Interaction Element for Dynamic Analysis," *Journal of Structural Engineering*, **123**, pp. 1512–1518 (1997).
2. Yang, Y. B., Yau, J. D. and Wu, Y. S., *Vehicle-Bridge Interaction Dynamics*, World Scientific, Singapore (2004).
3. Frýba, L., *Vibration of Solids and Structures Under Moving Loads*, 3rd Ed., Thomas Telford, London (1999).
4. Xia, H., Xu, Y. L. and Chan, T. H. T., "Dynamic Interaction of Long Suspension Bridges with Running Trains," *Journal of Sound and Vibration*, **237**, pp. 263–280 (2000).
5. Xia, H. and Zhang, N., "Dynamic Analysis of Railway Bridge Under High-Speed Trains," *Computer & Structures*, **83**, pp. 1891–1901 (2005).
6. Lou, P., "A Vehicle-Track-Bridge Interaction Element Considering Vehicle's Pitching Effect," *Finite Element Analysis and Design*, **41**, pp. 397–427 (2005).
7. Ju, S. H., Lin, H. T., Hsueh, C. C. and Wang, S. L., "A Simple Finite Element Model for Vibration Analyses Induced by Moving Vehicles," *International Journal for Numerical Method and Engineering*, **68**, pp. 1232–1256 (2006).
8. Ju, S. H. and Lin, H. T., "A Finite Element Model of Vehicle-Bridge Interaction Considering Braking and Acceleration," *Journal of Sound and Vibration*, **303**, pp. 46–57 (2007).
9. Xia, H., Guo, W. W., Wu, X., Pi, Y. L. and Bradford, M. A., "Lateral Dynamic Interaction Analysis of a

https://doi.org/10.1017/jmech.2014.89 Published online by Cambridge University Press

Train-Girder-Pier System," *Journal of Sound and Vibration*, **318**, pp. 927–942 (2008).
10. Liu, K., De Roeck, G. and Lombaert, G., "The Effect of Dynamic Train-Bridge Interaction on the Bridge Response During a Train Passage," *Journal of Sound and Vibration*, **325**, pp. 240–251 (2009).
11. Zhan, J. W., Xia, H., Chen, S. Y. and De Roeck, G., "Structural Damage Identification for Railway Bridges Based on Train-Induced Bridge Responses and Sensitivity Analysis," *Journal of Sound and Vibration*, **330**, pp. 757–770 (2011).
12. Yang, Y. and Fonder, G. A., "An Iterative Solution Method for Dynamic Response of Bridge Vehicles Systems," *Earthquake Engineering and Structural Dynamics*, **25**, pp. 195–215 (1996).
13. Ju, S. H. and Lin, H. T., "Numerical Investigation of a Steel Arch Bridge and Interaction with High-Speed Trains," *Engineering Structures*, **25**, pp. 241–250 (2007).
14. Zhang, N., Xia, H. and Guo, W. W., "Vehicle-Bridge Interaction Analysis under High-Speed Trains," *Journal of Sound and Vibration*, **309**, pp. 407–425 (2008).
15. Yau, J. D., "Vehicle/Bridge Interactions of a Rail Suspension Bridge Considering Support Movements," *Interaction and Multi-Scale Mechanics: An International Journal*, **2**, pp. 263–276 (2009).
16. Garg, V. K. and Dukkipati, R. V., *Dynamics of Railway Vehicle Systems*, Academic Press, New York (1984).
17. Yang, Y. B. and Lin, B. H., "Vehicle-Bridge Interaction Analysis by Dynamic Condensation Method," *Journal of Structural Engineering*, **121**, pp. 1636–1643 (1995).
18. Yang, Y. B., Chang, C. H. and Yau, J. D., "An Element for Analysing Vehicle-Bridge Systems Considering Vehicle's Pitching Effect," *International Journal for Numerical Method and Engineering*, **46**, pp. 1031–1047(1999).
19. Yang, Y. B. and Wu, Y. S., "A Versatile Element for Analyzing Vehicle-Bridge Interaction Response," *Engineering Structures*, **23**, pp. 452–469 (2001).
20. European Committee Forstandardization (CEN), *EN1991-2. Eurocode 1: Actions on Structures — Part 2: Traffic Loads on Bridges*, Brussels, Belgium (2003).
21. Yang, Y. B., Lin, C. W. and Yau, J. D., "Extracting Bridge Frequencies from the Dynamic Response of a Passing Vehicle," *Journal of Sound and Vibration*, **272**, pp. 471–493 (2004).
22. Yang, Y. B., Yau, J. D. and Hsu, L. C., "Vibration of Simple Beams due to Trains Moving at High Speeds," *Engineering Structures*, **19**, pp. 936–994(1997).
23. Ju, S. H. and Lin, H. T., "Resonance Characteristics of High-Speed Trains Passing Simply Supported Bridges," *Journal of Sound and Vibration*, **267**, pp. 1127–1141 (2003).
24. Xia, H., Zhang, N. and Guo, W. W., "Analysis of Resonance Mechanism and Conditions of Train-Bridge System," *Journal of Sound and Vibration*, **297**, pp. 810–822 (2006).
25. Mao, L. and Lu, Y., "Critical Speed and Resonance Criteria of Railway Bridge Response to Moving Trains," *Journal of Bridge Engineering*, **18**, pp. 131–141 (2013).
26. Museros, P., Moliner, E. and Martínez-Rodrigo M. D., "Free Vibrations of Simply-Supported Beam Bridges Under Moving Loads: Maximum Resonance, Cancellation and Resonant Vertical Acceleration," *Journal of Sound and Vibration*, **332**, pp. 326–345 (2013).
27. Doménech, A., Museros, P. and Martínez-Rodrigo M. D., "Influence of the Vehicle Model on the Prediction of the Maximum Bending Response of Simply-Supported Bridges Under High-Speed Railway Traffic," *Engineering Structures*, **72**, pp. 123–139 (2014).

(Manuscript received October 11, 2013,
accepted for publication August 27, 2014.)

https://doi.org/10.1017/jmech.2014.89 Published online by Cambridge University Press